The International Archives of the Photogrammetry, Remote Sensing and Spatial Information Sciences, Volume XLVIII-M-6-2025
ISPRS, EARSeL & DGPF Joint Istanbul Workshop "Topographic Mapping from Space" dedicated to Dr. Karsten Jacobsen's 80th Birthday
29–31 January 2025, Istanbul, Türkiye

Analysis of Coherence Between Linear and Cubic SBAS Displacement Models in Deformation Monitoring

Umut Gunes Sefercik [1], Mahmut Gorken [2], Mertcan Nazar [1]

[1] Department of Geomatics Engineering, Gebze Technical University, Kocaeli, Türkiye - sefercik@gtu.edu.tr, mnazar@gtu.edu.tr
[2] Department of Architecture and Urban Planning, Şefaatli Vocational School, Yozgat Bozok University, Yozgat, Türkiye - mahmut.gorken@bozok.edu.tr

Keywords: MT-InSAR, SBAS, Displacement Model, Deformation Monitoring, Reclamation Area, Coherence Analysis.

Abstract

Land reclamation projects are a common feature of coastal cities around the world and have been carried out for a number of different purposes. The rapid growth of the global population and the concomitant increase in socioeconomic developments have resulted in a corresponding rise in demand for air transportation services. The construction of airports on reclaimed areas may result in an increased susceptibility to ground subsidence, which could potentially lead to damage to the infrastructure and safety concerns for the public. Consequently, traditional ground deformation methodologies have been extensively employed in small-scale applications, although their spatial resolution is restricted and they require a considerable input of labor and time. In order to monitor ground deformation at reclaimed airports, interferometric synthetic aperture radar (InSAR) technology has become an invaluable tool. Furthermore, the small baseline subset (SBAS) method, a multi-temporal InSAR (MT-InSAR) approach, was developed for the periodic monitoring of ground deformation with sub-centimeter accuracy. This was achieved through the utilization of a SAR dataset with small baselines, thereby enhancing the quality of interferograms. The present study comprises a coherence analysis of linear and cubic SBAS displacement models, with ground deformation monitoring at Hatay Airport based on 151 Sentinel-1A single-look complex (SLC) SAR images acquired between 2 December 2017 and 29 January 2023. Consequently, the mean deformation velocity and the cumulative deformation values were determined in the satellite line-of-sight (LOS) direction. Cumulative vertical deformation maps were generated for both the linear and cubic SBAS displacement models, with values ranging from -142.71 mm to 60.11 mm and from -224.84 mm to 69.9 mm, respectively. The coherence analysis yielded a standard deviation of ±8.525 mm after bias elimination, for the differences in cumulative vertical deformation between the linear and cubic SBAS displacement models. A cumulative vertical deformation difference map was ultimately constructed, with values ranging from -42 mm to 42 mm.

1. Introduction

In numerous coastal cities across the globe, land reclamation projects have been initiated for a multitude of purposes. Until the last two decades, coastal reclamation projects were mostly undertaken by a limited number of countries, including the USA, the Netherlands, China, South Korea, Singapore, and Japan (Sengupta et al., 2023). Population growth and socioeconomic development have increased the demand for air transport services, stimulating airport construction projects in reclaimed areas (Zhao et al., 2011; Liu et al., 2019). However, airports constructed on reclaimed land may be susceptible to subsidence, deformation, and cracking (Bao et al., 2022). Traditional ground deformation monitoring methods have been employed, yet they offer limited resolution and can be costly and time-consuming (Jiang et al., 2016).

Interferometric synthetic aperture radar (InSAR) has become an invaluable tool for monitoring large-scale ground deformation in reclaimed airports over extended time periods. Furthermore, multi-temporal InSAR (MT-InSAR) methods were developed for the monitoring of ground deformation over extended periods of time, with an accuracy level of sub-centimetres. Accordingly, the small baseline subset (SBAS) method has been developed to periodically detect ground deformation by using SAR acquisitions with minimal orbital differences to improve the quality of the generated interferograms (Berardino et al., 2002). SBAS, initially intended for detecting large-scale deformations of 100 m x 100 m, has been improved through the integration of two separate SAR datasets, comprising both multilook and single-look datasets, to evaluate the temporal evolution of local deformation patterns (Lanari et al., 2004). Despite employing a SAR dataset characterized by low temporal and spatial baselines, the SBAS method faces constraints, particularly due to the typically non-homogeneous distribution of scatterers among different land use land cover classes (LULC) (Lanari et al., 2007).

It is acknowledged that atmospheric phase delay error has the potential to impact the accuracy of InSAR measurements, consequently affecting the precision of deformation monitoring results. In light of this, a range of atmospheric correction methodologies have been developed, including the Generic Atmospheric Correction Online Service for InSAR (GACOS), which employs the Iterative Tropospheric Decomposition (ITD) model (Yu et al., 2018a; Yu et al., 2018b). Applications of SBAS include urban subsidence monitoring (Wu et al., 2019), deformation estimation in volcanic areas (Babu and Kumar, 2019), glacier deformation detection (Du et al., 2020), landslide susceptibility mapping (Zhao et al., 2019), mapping coseismic deformations (Lanari et al., 2010), structural monitoring (Arangio et al., 2014), and airport deformation monitoring (Sefercik et al., 2024).

Surface deformation phenomena can display unique spatial and temporal patterns. This can subsequently affect the SBAS InSAR time series results. Various SBAS polynomial models including linear, quadratic, cubic, and linear periodic are utilized to align with the examined deformation patterns more effectively. The initial SBAS method was structured on the linear displacement model to analyze surface deformation (Li et al., 2022). Different polynomial models have been employed in various instances, particularly those involving non-linear deformation (Zhang et al., 2012; Zhao et al., 2016). It is therefore imperative to select the optimal polynomial displacement model to effectively analyze the deformation mechanics of the investigated area.

In this study, a coherence analysis of linear and cubic SBAS displacement models based on cumulative vertical deformation values was performed to monitor ground deformation at the reclaimed Hatay Airport area. The analysis was based on 151 Sentinel-1A single-look complex (SLC) images obtained between 2 December 2017 and 29 January 2023. During the analysis, an atmospheric phase delay correction was performed based on data provided by the GACOS system.

2. Study Area and Dataset

Hatay Airport was situated in Hatay, Turkey, at 36°21'46.0"N and 36°16'56.0"E. The total area was approximately 2.70 km², comprising a total terminal area of 46826 m² and a single concrete runway measuring 3000 m x 45 m. The airport, officially opened in 2007, was built on the basin of the formerly existing Lake Amik. The region is currently characterized by agricultural land and rural centers. The Hatay Airport area is presented in Figure 1.

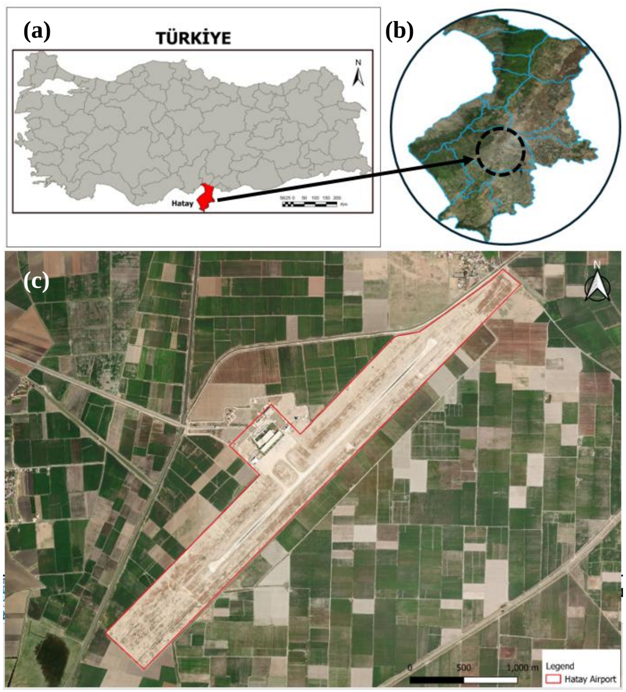

Figure 1. (a) Location of Hatay in Turkey, (b) Hatay regional map showing the location of the airport in circle, and (c) Hatay Airport area.

The area of interest has a documented history of flooding events along with the existence of reclaimed land that may increase susceptibility to land subsidence. The Sentinel-1A SLC dataset, comprising 151 SAR images captured between 2 December 2017 and 29 January 2023, was obtained in interferometric wide swath (IW) mode, descending orbit, and vertical-vertical (VV) polarization. The Sentinel-1A SLC images was acquired using the Alaska Satellite Facility's (ASF) Vertex Platform. The features of the utilized Sentinel-1A dataset are presented in Table 1.

Feature	Description
Product	Sentinel-1A TOPS SLC
Band/Wavelength	C-band/5.55 cm
Acquisition period	20171202-20230129
Total image number	151
Acquisition mode	IW
Orbit	Descending
Polarization	VV
Path/Frame No.	21/14
Spatial resolution	Ground range 5 m x Azimuth 20 m
Pixel spacing	Slant range 2.3 m x Azimuth 14.1 m
Incidence angle	29°-46°
Total swath width	250 km
Revisit period	12 days

Table 1. The features of the utilized Sentinel-1A dataset.

3. Methodology

The processing of SBAS for this study was carried out in accordance with the methodologies detailed in the SARscape SBAS tutorial manual (version 5.6.2) (SARMAP, 2022). The processing of SBAS was carried out utilizing the SARscape 5.6.2.1 software specifically designed for SAR processing, which is incorporated within the ENVI 5.6.3 software suite. The procedural stages encompassed in SBAS consist of the formulation of a connection graph, the identification of an optimal master image, coregistration and phase unwrapping, the execution of refinement and flattening, the initiation of a first inversion alongside the determination of the displacement model type, a subsequent inversion, the application of GACOS data for atmospheric phase delay correction, and the process of geocoding. The super master image was established on 12 August 2020, with the remaining slave images coregistered to this master (Figure 2).

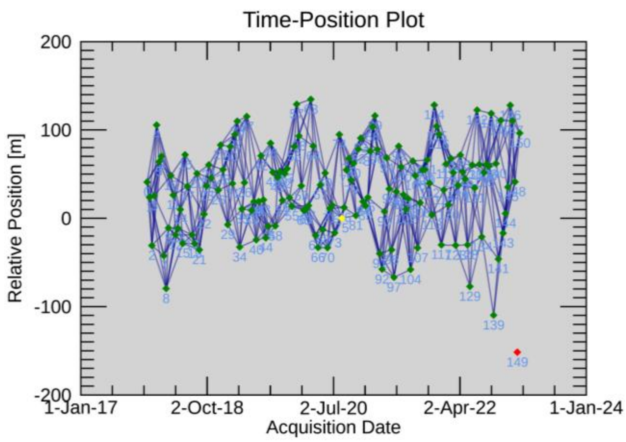

Figure 2. The connection graph showing the relative position of images to selected super master image in yellow and acquisition dates. One image shown in red was discarded due to baseline threshold.

Deformation may arise from a range of natural or human-induced events and can exhibit both linear and non-linear trends over time. The choice of a suitable displacement model is essential for analyzing the SBAS deformation time series. SARscape comprises four distinct SBAS displacement models: linear, quadratic, cubic, and linear periodic. The equation representing the three displacement polynomial models including linear, quadratic, and cubic can be expressed as follows:

$$Disp = K_1(t - t_0) + \frac{1}{2}K_2(t - t_0)^2 + \frac{1}{6}K_3(t - t_0)^3 \quad (1)$$

where $Disp$ is the displacement at time t, K_1 is the linear term (mm/year) representing the instantaneous displacement velocity, K_2 is the quadratic term (mm/year^2) representing the instantaneous acceleration, K_3 is the cubic term (mm/year^3) representing the instantaneous acceleration variation. In addition, the linear periodic model can be defined as follows:

$$Disp = K_1(t - t_0) + K_2\cos(2\pi F(t - t_0) + K_3) \quad (2)$$

where $Disp$ the displacement at time t, K_1 is the linear term (mm/year) representing the instantaneous displacement velocity, K_2 is the modulation term (mm), K_3 is the delay (days), and F is the known expected frequency (1/Model Period). The application of SBAS method generates displacement data along the satellite LOS and this can be decomposed into distinct components in both horizontal and vertical planes. The three-dimensional (3D) decomposition of the displacement vector can be expressed as follows:

$$\begin{aligned} d_r = d_u\cos(\theta_{inc}) - \sin(\theta_{inc})\Big[d_n\cos\Big(\alpha_h - \frac{3\pi}{2}\Big) \\ + d_e\sin\Big(\alpha_h - \frac{3\pi}{2}\Big)\Big] \end{aligned} \quad (3)$$

where d_r is the slant-range displacement in the LOS direction, d_u is the vertical displacement in the up-down direction, d_n is the horizontal displacement in the north-south direction, d_e is the horizontal displacement in the east-west direction of 3D displacement vector $\vec{d}$, θ_{inc} is the angle of incidence and α_h is the heading angle (Hanssen, 2001). In order to obtain cumulative vertical deformation values, the slant displacement in the LOS direction was converted to displacement in the up-down direction. The cosine correction technique was utilized to derive the vertical deformation in the up-down direction, based on the assumption of exclusive vertical movement, with no horizontal displacement (Bayramov et al., 2021). Cosine correction can be defined as the following equation (Yang et al., 2019).

$$d_u = \frac{d_r}{\cos(\theta_{inc})} \quad (4)$$

Using the cumulative vertical deformation values a vector-to-raster transformation was executed in Surfer software based on nearest neighbour interpolation and 5 m grid spacing. Following this, a coherence analysis was conducted between cumulative vertical deformation raster maps of linear and cubic SBAS displacement models using the BLUH system from Leibniz University Hannover, employing the standard deviation metric. The generation of maps was performed using the QGIS 3.32.3 software.

4. Results

Cumulative vertical deformation maps of linear and cubic SBAS displacement models are shown in Figure 3.

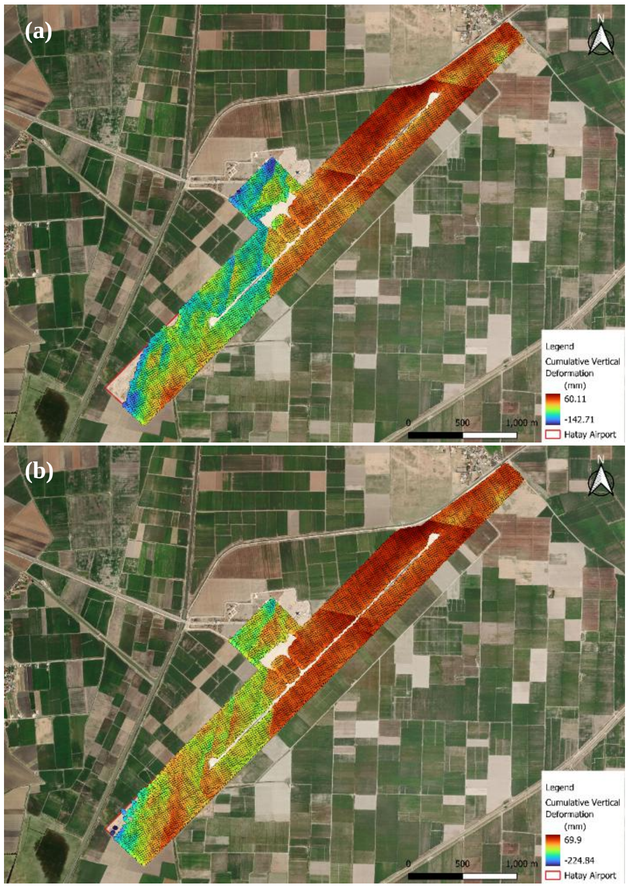

Figure 3. Cumulative vertical deformation maps: (a) linear and (b) cubic SBAS displacement models.

The cumulative vertical deformation values for the linear and cubic SBAS displacement models exhibited a range from -142.71 mm to 60.11 mm and from -224.84 mm to 69.9 mm, respectively. In the northern sector of the airport, the aggregated vertical deformation measurements predominantly exhibited positive values across both models, suggesting a possible trend of uplift in the area. Conversely, the cumulative vertical deformation values predominantly exhibited negative values on the southern side for both models, indicating a possible trend of subsidence in the region. The aggregate count of scatterer points for the linear and cubic SBAS displacement models was recorded as 11,244 and 11,360, respectively. A notable decrease in the density of scatterer points was recorded in both the runway and terminal regions. Furthermore, in the southwestern region, especially concerning the linear SBAS displacement model. The lack of coherence can be ascribed to the geometry of the objects, the characteristics of the topography, and the presence of incoherent differential interferogram pairs. The findings from the coherence analysis pertaining to the linear and cubic SBAS displacement models are presented in Table 2.

Standard deviation (mm)		
CM \ REF	Linear	Cubic
Linear	0.000	8.525 (EB=8.452)
Cubic	8.525 (EB=-8.452)	0.000

Table 2. The results of the coherence analysis of the linear and cubic SBAS displacement models (CM=Compared model, REF=Reference model, EB=Eliminated bias).

The standard deviation of the SBAS displacement models was determined to be 8.525 mm subsequent to the elimination of a bias measured at 8.452 mm. The elimination of bias represents an essential phase in the execution of a precise coherence analysis. Figure 4 presents the histogram illustrating the frequency and standard deviation of the cumulative vertical deformation difference values.

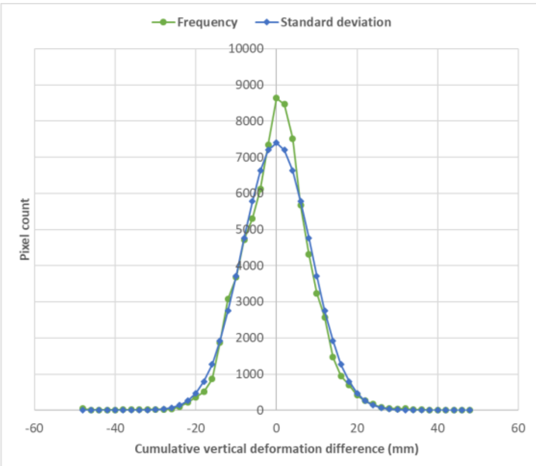

Figure 4. The frequency and standard deviation histogram of the cumulative vertical deformation difference values.

The histogram depicting frequency and standard deviation reveals a discernible normal distribution of cumulative vertical deformation differences. Figure 5 illustrates the cumulative vertical deformation difference map derived from the linear and cubic SBAS displacement models.

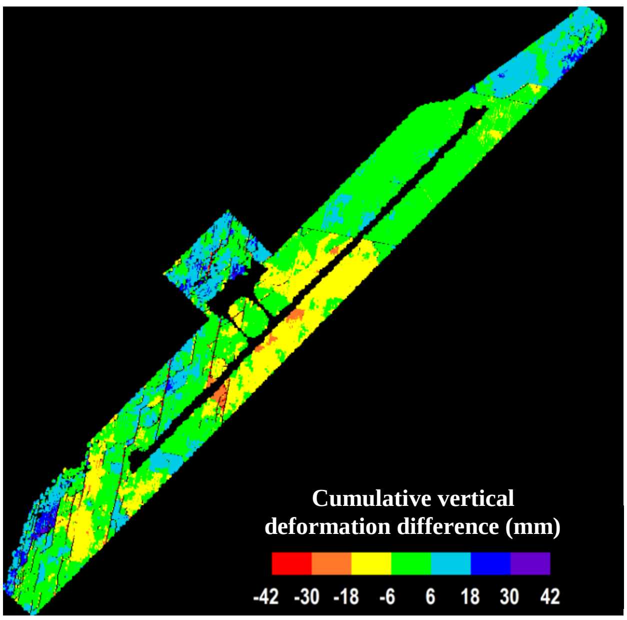

Figure 5. Cumulative vertical deformation difference map.

The recorded cumulative vertical deformation difference demonstrated a variation spanning from -42 mm to 42 mm. Nevertheless, the observed cumulative vertical deformation differences for both the linear and quadratic SBAS displacement models were primarily found to attain a maximum of ±18 mm. The cumulative vertical deformation differences predominantly ranged around ±6 mm, with values notably concentrated between -6 mm and -18 mm, particularly in the central section of the airport.

5. Conclusions

The creation of an airport in reclaimed areas could expose the facility to risks associated with subsidence and possible deterioration of infrastructure. Therefore, it is imperative to monitor ground deformation to guarantee the ongoing operation of airports and the overall safety of the public. In conjunction with traditional terrestrial methods, the InSAR technique is employed for the accurate observation of ground deformation, attaining measurements with millimeter precision. The SBAS method, classified as a variant of MT-InSAR, is employed for the systematic observation of ground deformation attributable to reclamation activities within airport zones. This research employed coherence analysis of linear and quadratic SBAS displacement models to systematically observe ground deformation at Hatay Airport. In pursuit of this objective, a comprehensive analysis was conducted utilizing a total of 151 Sentinel-1A SLC SAR images, which were acquired between 2 December 2017 and 29 January 2023, to effectively detect ground deformation within an airport area that experienced reclamation activities. The cumulative vertical deformation for the linear and cubic SBAS displacement models was found to vary from -142.71 mm to 60.11 mm and from -224.84 mm to 69.9 mm, respectively. A transformation from vector to raster was employed to conduct a coherence analysis of cumulative vertical deformation maps obtained from both linear and quad SBAS displacement models. Following the elimination of bias, the standard deviation of the differences noted in cumulative vertical deformation values was determined to be ±8.525 mm. A cumulative vertical deformation difference map was generated to compare linear and quadratic SBAS displacement models, with values ranging from -42 mm to 42 mm. In the vicinity of the airport, the maximum cumulative vertical deformation difference was primarily recorded at ±18 mm. While the cumulative vertical deformation differences observed between the linear and quadratic SBAS displacement models were relatively minor, measuring under one centimeter in certain areas, there were instances where these discrepancies became markedly more pronounced. The choice of a displacement model has been demonstrated to have a substantial effect on the outcomes of deformation monitoring, especially within the framework of reclaimed airport regions. The SBAS method demonstrates considerable promise for the observation of deformation in reclaimed airports, potentially aiding in hazard mitigation and the improvement of safety protocols. Furthermore, the results obtained from SBAS deformation monitoring can be employed within a more comprehensive framework to facilitate the identification of potential hazards and the evaluation of the structural integrity of engineering constructions in reclaimed areas.

References

Arangio, S., Calò, F., Di Mauro, M., Bonano, M., Marsella, M., Manunta, M., 2014. An application of the SBAS-DInSAR technique for the assessment of structural damage in the city of Rome. *Structure and Infrastructure Engineering*, 10(11), 1469-1483. doi.org/10.1080/15732479.2013.833949.

Babu, A., Kumar, S., 2019. SBAS interferometric analysis for volcanic eruption of Hawaii Island. *Journal of Volcanology and Geothermal Research*, 370, 31-50. doi.org/10.1016/j.jvolgeores.2019.01.011.

Bao, X., Zhang, R., Shama, A., Li, S., Xie, L., Lv, J., Fu, Y., Wu, R., Liu, G., 2022. Ground deformation pattern analysis and evolution prediction of Shanghai Pudong International Airport based on PSI long time series observations. *Remote Sensing*, 14(3), 610. doi.org/10.3390/rs14030610.

Berardino, P., Fornaro, G., Lanari, R., Sansosti, E., 2002. A new algorithm for surface deformation monitoring based on small baseline differential SAR interferograms. *IEEE Transactions On Geoscience and Remote Sensing*, 40(11), 2375-2383. doi.org/10.1109/TGRS.2002.803792.

Bayramov, E., Buchroithner, M., Kada, M., Zhuniskenov, Y., 2021. Quantitative assessment of vertical and horizontal deformations derived by 3D and 2D decompositions of InSAR line-of-sight measurements to supplement industry surveillance programs in the Tengiz Oilfield (Kazakhstan). *Remote Sensing*, 13(13), 2579. doi.org/10.3390/rs13132579.

Du, W., Ji, W., Xu, L., Wang, S., 2020. Deformation time series and driving-force analysis of glaciers in the Eastern Tienshan Mountains using the SBAS InSAR method. *International Journal of Environmental Research and Public Health*, 17(8), 2836. doi.org/10.3390/ijerph17082836.

Hanssen, R.F., 2001. *Radar Interferometry: Data Interpretation and Error Analysis*. Kluwer Academic Publishers, Dordrecht, The Netherlands.

Jiang, Y., Liao, M., Wang, H., Zhang, L., Balz, T., 2016. Deformation monitoring and analysis of the geological environment of Pudong International Airport with persistent scatterer SAR interferometry. *Remote Sensing*, 8(12), 1021. doi.org/10.3390/rs8121021.

Lanari, R., Berardino, P., Bonano, M., Casu, F., Manconi, A., Manunta, M., Manzo, M., Pepe, A., Pepe, S., Sansosti, E., Solaro, G., 2010. Surface displacements associated with the L'Aquila 2009 Mw 6.3 earthquake (central Italy): New evidence from SBAS-DInSAR time series analysis. *Geophysical Research Letters*, 37, L20309. doi.org/10.1029/2010GL044780.

Lanari, R., Casu, F., Manzo, M., Zeni, G., Berardino, P., Manunta, M., Pepe, A., 2007. An overview of the small baseline subset algorithm: A DInSAR technique for surface deformation analysis. *Pure and Applied Geophysics*, 164(4), 637-661. doi.org/ 10.1007/s00024-007-0192-9.

Lanari, R., Mora, O., Manunta, M., Mallorquí, J.J., Berardino, P., Sansosti, E., 2004. A small-baseline approach for investigating deformations on full-resolution differential SAR interferograms. *IEEE Transactions on Geoscience and Remote Sensing*, 42(7), 1377-1386. doi.org/10.1109/TGRS.2004.828196.

Li, S., Xu, W., Li, Z., 2022. Review of the SBAS InSAR time-series algorithms, applications, and challenges. *Geodesy and Geodynamics*, 13(2), 114-126. doi.org/10.1016/j.geog.2021.09.007.

Liu, X., Zhao, C., Zhang, Q., Yang, C., Zhang, J., 2019. Characterizing and monitoring ground settlement of marine reclamation land of Xiamen New Airport, China with Sentinel-1 SAR datasets. *Remote Sensing*, 11(5), 585. doi.org/10.3390/rs11050585.

SARMAP, 2022. SARscape SBAS Tutorial Manual, Version 5.6.2. sarmap.ch/tutorials/SBAS_Tutorial_562.pdf (25 December 2024).

Sefercik, U.G., Nazar, M., Gorken, M., 2024. Coherence analysis of small baseline subset displacement model types in deformation monitoring. *Proceedings of the 45th Asian Conference on Remote Sensing*, 1-14.

Sengupta, D., Choi, Y.R., Tian, B., Brown, S., Meadows, M., Hackney, C.R., Banerjee, A., Li, Y., Chen, R., Zhou, Y., 2023. Mapping 21st century global coastal land reclamation. *Earth's Future*, 11(2), e2022EF002927. doi.org/10.1029/2022EF002927.

Wu, Q., Jia, C., Chen, S., Li, H., 2019. SBAS-InSAR based deformation detection of urban land, created from mega-scale mountain excavating and valley filling in the Loess Plateau: The case study of Yan’an City. *Remote Sensing*, 11(14), 1673. doi.org/10.3390/rs11141673.

Yang, Y.J., Hwang, C., Hung, W.C., Fuhrmann, T., Chen, Y.A., Wei, S.H., 2019. Surface deformation from Sentinel-1A InSAR: Relation to seasonal groundwater extraction and rainfall in Central Taiwan. *Remote Sensing*, 11(23), 2817. doi.org/10.3390/rs11232817.

Yu, C., Li, Z., Penna, N.T., 2018a. Interferometric synthetic aperture radar atmospheric correction using a GPS-based iterative tropospheric decomposition model. *Remote Sensing of Environment*, 204, 109-121. doi.org/10.1016/j.rse.2017.10.038.

Yu, C., Li, Z., Penna, N.T., Crippa, P., 2018b. Generic atmospheric correction model for interferometric synthetic aperture radar observations. *Journal of Geophysical Research: Solid Earth*, 123(10), 9202-9222. doi.org/10.1029/2017JB015305.

Zhang, Y., Wu, H. A., Sun, G., 2012. Deformation model of time series interferometric SAR techniques. *Acta Geodaetica et Cartographica Sinica*, 41(6), 864-869.

Zhao, F., Meng, X., Zhang, Y., Chen, G., Su, X., Yue, D., 2019. Landslide susceptibility mapping of Karakorum highway combined with the application of SBAS-InSAR technology. *Sensors*, 19(12), 2685. doi.org/10.3390/s19122685.

Zhao, Q., Lin, H., Gao, W., Zebker, H.A., Chen, A., Yeung, K., 2011. InSAR detection of residual settlement of an ocean reclamation engineering project: A case study of Hong Kong International Airport. *Journal of Oceanography*, 67, 415-426. doi.org/10.1007/s10872-011-0034-3.

Zhao, R., Li, Z.W., Feng, G.C., Wang, Q.J., Hu, J., 2016. Monitoring surface deformation over permafrost with an improved SBAS-InSAR algorithm: With emphasis on climatic factors modeling. *Remote Sensing of Environment*, 184, 276-287. doi.org/10.1016/j.rse.2016.07.019.